INTRODUCTION

The aim of this project is to investigate the Static Stability of the three-bar rigid linkage shown in figure 1. The analysis of the system is carried out by:

1. Formulating the Energy Function of the structure from which the Virtual Work function and the Hessian matrix are derived.
2. Solving the Equilibrium equations obtained from the Virtual work function using Newton's Algorithm (with arc-length constraint).
3. Locating the points of Bifurcation and tracing the Equilibrium Path (Bifurcation Diagram) of the system.
4. Finally, examining the effect of geometric imperfections on the stability and the Bifurcation Diagram of the system.

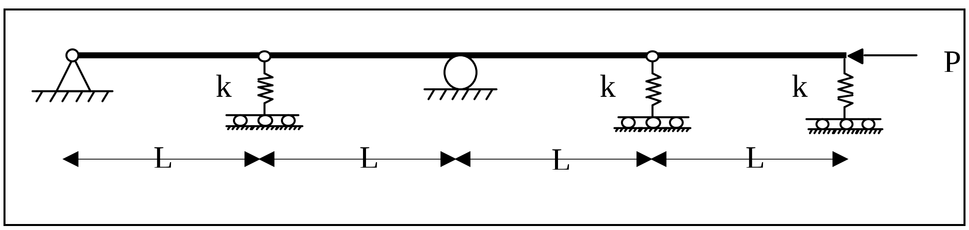

Fig 1: Two degree of freedom system chosen for this project.

DOF OF THE STRUCTURE

The given system has two degrees of freedom. The system can deform in four possible ways, by different combinations of the rotations of the hinges and elongation (or compression) of the springs. In this project, for ease of formulating the equations, the rotation of the hinges (θ_1,θ_2) are used to represent the deformation of the system as shown in Figure 2.

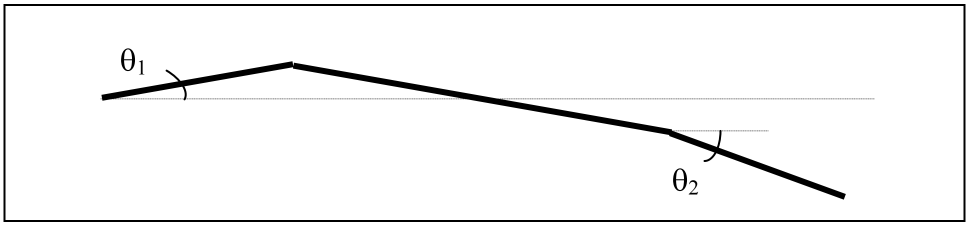

Fig 2: Convenient choice of degrees of freedom and representation of deformation.

ENERGY FUNCTION

The potential energy of the system in the deformed configuration is given by:

$$\xi(\theta_1, \theta_2) = 2(\mathrm{K}/2)(\mathrm{L}Sin\theta_1)^2 + (\mathrm{K}/2)(\mathrm{L}Sin\theta_1 + \mathrm{L}Sin\theta_2)^2 + \mathrm{P}(3\mathrm{L}Cos\theta_1 + \mathrm{L}Cos\theta_2)$$

Simplifying the above expression gives the energy function of the system: equation (1).

$$\xi(\theta_1, \theta_2) = (\mathrm{KL}^2/2)(3Sin^2\theta_1 + 2Sin\theta_1 Sin\theta_2 + Sin^2\theta_2) + \mathrm{PL}(3Cos\theta_1 + Cos\theta_2) \rightarrow (1)$$

VIRTUAL WORK FUNCTION

The virtual work function of the system, equation (2) is obtained by taking the directional directive of the Energy function i.e. differentiating equation (1) first with respect to θ_1 and then with respect to θ_2.

$$\mathrm{G}(\theta_1, \bar{\theta}_1, \theta_2, \bar{\theta}_2) = \begin{matrix} \left[(\mathrm{KL}^2)(3Sin\,\theta_1 Cos\,\theta_1 + Cos\,\theta_1 Sin\,\theta_2) - 3\mathrm{PL}\,Sin\,\theta_1\right]\bar{\theta}_1 + \\ \left[(\mathrm{KL}^2)(Sin\,\theta_1 Cos\,\theta_2 + Sin\,\theta_2 Cos\,\theta_2) - \mathrm{PLSin}\,\theta_2\right]\bar{\theta}_2 \end{matrix} \rightarrow (2)$$

Where $\bar{\theta}_1, \bar{\theta}_2$ are the virtual displacements

EQUATIONS OF EQUILIBRIUM

The equations of equilibrium are obtained by applying the fundamental theorem of the calculus of variations to the virtual work function. Thus,

$$(\mathrm{KL}^2)(3Sin\theta_1 Cos\theta_1 + Cos\theta_1 Sin\theta_2) - 3\mathrm{PL}Sin\theta_1 = 0 \rightarrow (3)$$
$$(\mathrm{KL}^2)(Sin\theta_1 Cos\theta_2 + Cos\theta_2 Sin\theta_2) - \mathrm{PL}Sin\theta_2 = 0 \quad \rightarrow (4)$$

Dividing equation (3) throughout by $\mathrm{KL}^2 Cos\theta_1$ and equation (4) throughout by $\mathrm{KL}^2 Cos\theta_2$ to get:

$$3Sin\theta_1 + Sin\theta_2 - 3pTan\theta_1 = 0 \rightarrow (5)$$
$$Sin\theta_1 + Sin\theta_2 - pTan\theta_2 = 0 \quad \rightarrow (6)$$
$$\text{where}: p = \mathrm{P}/(\mathrm{KL})$$

These equations are system of two non-linear algebraic equations in the unknowns θ_1 and θ_2 for a given value of load parameter *p*. Solution of these equations for different values of *p* gives the equilibrium path (or Bifurcation Diagram) for the system. Since, the system has two degrees of freedom, it has multiple equilibrium paths.

HESSIAN MATRIX

The second derivative of the Energy Equation gives the Hessian Matrix for the system.

$$\mathrm{A}(\theta, p) = \begin{bmatrix} 3Cos\theta_1 - 3pSec^2\theta_1 & Cos\theta_2 \\ Cos\theta_1 & Cos\theta_2 - pSec^2\theta_2 \end{bmatrix}$$

The stability of the system will be judged by the sign of the eigen values of the Hessian Matrix at an equilibrium configuration.

EQUILIBRIUM PATH OF SYSTEM WIHOUT IMPERFECTIONS

Clearly, the straight configuration, $\theta^T=\{0,0\}$, satisfies the equilibrium equations and is a solution for all values of the load parameter *p*. The stability can be judged by the eigenvalues of the Hessian matrix. A straightforward computation shows that these eigenvalues are given by:

$$\lambda_1 = 2\alpha - \sqrt{(\alpha^2 + 1)}\ ,\ \lambda_2 = 2\alpha + \sqrt{(\alpha^2 + 1)} \qquad \text{where}: \alpha = (1 - p)$$

The system will be stable only if both eigenvalues λ_1 and λ_2 are positive. λ_1 remains positive for $p < (1 - 1/\sqrt{3}) = 0.423$ and λ_2 is positive for $p < (1 + 1/\sqrt{3}) = 1.577$, indicating that system is stable if $p < 0.423$ and unstable if $p > 0.423$. Thus, in this configuration the structure can comfortably sustain a load of magnitude P = 0.423KL and loads greater than this provided the structure is restrained against buckling and barring any initial imperfections. It can also be observed, that the structure will be inherently stable for negative values of P (tensile loads).

The Bifurcation points lie on the branch $\theta_1 = \theta_2 = 0$ and their exact positions can be obtained by observing where the eigenvalues of the Hessian matrix change sign as the load P increases in the positive direction (compressive). When the load P = 0, the eigenvalues are $\lambda_1 = 0.586$, $\lambda_2 = 3.414$ and they progressively keep on decreasing as the load P increases. At P = 0.423KL, λ_1 becomes zero and this represents the first bifurcation point, the boundary between stable and unstable behavior in the straight configuration. Beyond this point the structure cannot remain stable in the straight configuration and to gain stability must change into a bent configuration, the first buckling mode (figure 3), represented by branch 1 on the Bifurcation diagram (figure 5).

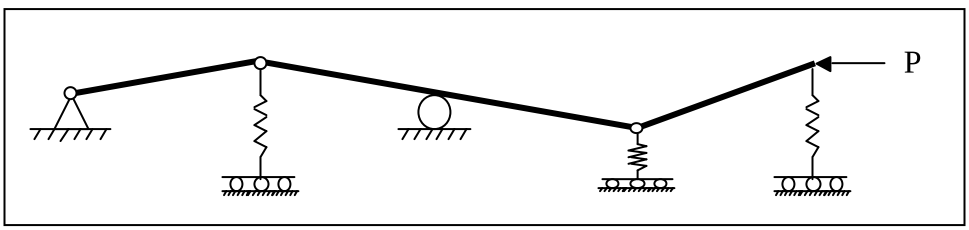

Fig 3: First buckling mode shape

The Branch 1 can be traced by solving the equilibrium equations iteratively by arc-length method. We know that the branch 1 starts at $\theta_1 = \theta_2 = 0$, $p = 0.423$ and the first eigen vector {0.5, -0.866) is tangent to it at that point. Thus, to generate branch 1 the computations are started at $\theta_1 = \theta_2 = 0$, $p = 0.423$ and initiated to go in the direction of the first eigen vector. The program NEWTON has been modified and coded in MATLAB to perform computations. The program code used to perform the computation has been included in the appendix.

The structure can be made to sustain loads greater than P=0.423KL if it is suitably restrained. If the load P is increased beyond 0.423KL in the straight configuration, λ_1 becomes negative and gets increasingly negative, however λ_2 still remains positive but continues to decrease. At P = 1.577KL, the second eigenvalue λ_2 becomes zero and this represents the second bifurcation point. At this point too the system tries to gain stability by changing into bent configuration, the second buckling mode (figure 4), represented by branch 2 on the bifurcation diagram. The system can sustain loads greater than 1.577KL if both the hinges are prevented from rotating.

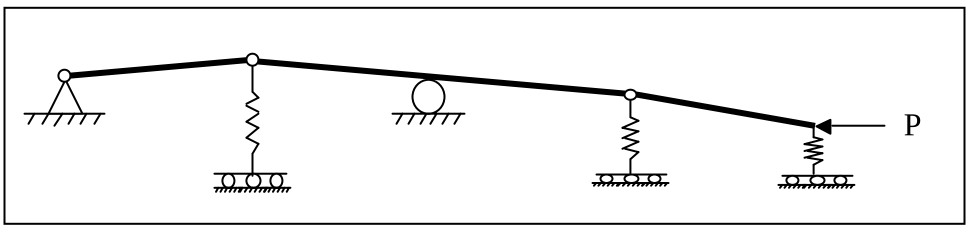

Fig 4: Second buckling mode shape

The Branch 2 can be traced by solving the equilibrium equations iteratively by arc-length method. We know that the branch 2 starts at $\theta_1 = \theta_2 = 0$, $p = 1.577$ and the second eigen vector {0.866, 0.5} is tangent to it at that point. Thus, to generate branch 2 the computations are started at $\theta_1 = 0$, $\theta_2 = 0$, $p = 1.577$ and initiated to go in the direction of second eigen vector.

The computations for branch 1 have been presented in Table 1. The Branch 1 has also been represented on the Bifurcation Diagram in figure 5. From the Bifurcation diagram, it is observed that the structure has to shed load after the first bifurcation point in order to maintain equilibrium in any point on the branch. As the deformations in Branch 1 increase, the capacity of the structure to carry load keeps on decreasing. Also, from table

1, it is observed that for Branch 1 the first eigen value is always negative, indicating that the system is unstable throughout the Branch 1.

ArcLength	0.05		
Initial θ_1	0	Next θ_1	0.5
Initial θ_2	0	Next θ_2	-0.86603
Initial *p*	0.42265	Next *p*	0.42265

N	θ_1	θ_2	*p*	λ_2	λ_1
1	0	0	0.42265	2.309401	0
2	0.025	-0.0433	0.4226	2.3071	-0.0012
3	0.0499	-0.0866	0.4216	2.303	-0.0032
4	0.0748	-0.13	0.4203	2.295	-0.0072
5	0.0994	-0.1735	0.4184	2.2839	-0.0128
6	0.1239	-0.217	0.416	2.2698	-0.02
7	0.1481	-0.2607	0.4131	2.2529	-0.029
8	0.1719	-0.3045	0.4097	2.2332	-0.0396
9	0.1953	-0.3485	0.4057	2.2111	-0.0522
10	0.2182	-0.3927	0.4011	2.1868	-0.0666
11	0.2406	-0.4371	0.396	2.1605	-0.0831
12	0.2623	-0.4818	0.3904	2.1327	-0.1018
13	0.2831	-0.5268	0.3841	2.1039	-0.123
14	0.3031	-0.5722	0.3773	2.0746	-0.147
15	0.322	-0.6178	0.3698	2.0456	-0.1741
16	0.3397	-0.6639	0.3617	2.0176	-0.205
17	0.3561	-0.7103	0.3529	1.9915	-0.2404
18	0.3709	-0.7571	0.3433	1.9686	-0.2811
19	0.384	-0.8042	0.3329	1.9499	-0.3283
20	0.3952	-0.8516	0.3217	1.9369	-0.3836
21	0.4043	-0.8993	0.3095	1.9308	-0.4487

Table 1: Results of computation for first buckling mode

The computations for branch 2 have been presented in Table 2. The Branch 2 has also been represented on the Bifurcation Diagram in figure 5. As seen from the diagram, the behavior of branch 2 is identical to that of Branch 1. The system has to shed load to maintain equilibrium at any point on the branch. Also, from the table it can seen that for Branch 2 both the eigen values are negative, suggesting that the system is unstable through out Branch 2.

ArcLength	0.05		
Initial θ_1	0	Next θ_1	0.866025
Initial θ_2	0	Next θ_2	0.5
Initial *p*	1.57735	Next *p*	1.57735

N	θ_1	θ_2	*p*	λ_1	λ_2
1	0	0	1.57735	-2.3094	0
2	0.025	0.0433	1.5764	-2.3133	-0.003
3	0.05	0.0865	1.5734	-2.313	-0.0118
4	0.0752	0.1294	1.5685	-2.3176	-0.0266
5	0.1004	0.1721	1.5617	-2.3243	-0.0473
6	0.1257	0.2143	1.5531	-2.3332	-0.0738
7	0.1512	0.256	1.5427	-2.3446	-0.1062
8	0.1769	0.2972	1.5306	-2.3589	-0.1444
9	0.2027	0.3377	1.5168	-2.3762	-0.1884
10	0.2288	0.3775	1.5015	-2.397	-0.2383
11	0.2551	0.4166	1.4848	-2.4216	-0.294
12	0.2817	0.4549	1.4667	-2.4503	-0.3556
13	0.3085	0.4924	1.4472	-2.4836	-0.4232
14	0.3356	0.529	1.4266	-2.5218	-0.4967
15	0.3628	0.5648	1.4048	-2.5653	-0.5762
16	0.3904	0.5997	1.382	-2.6144	-0.6619
17	0.4181	0.6338	1.3582	-2.6696	-0.7539
18	0.4461	0.6671	1.3334	-2.7312	-0.8523
19	0.4742	0.6995	1.3078	-2.7995	-0.9572
20	0.5025	0.7311	1.2814	-2.8751	-1.0688
21	0.531	0.762	1.2542	-2.9583	-1.1874

Table 2: Results of computation for second buckling mode

From figure 5 it is apparent that the system is unstable over majority of the bifurcation diagram. In fact, it never regains stability once it crosses the first Bifurcation point (i.e. for $P > 0.423$ KL). Thus, in no case should the load P be allowed to exceed 0.423KL.

EFFECT OF IMPERFECTIONS

Since, the structure is unstable over both the Bifurcation Branches and stable only for loads lesser than 0.423KL, the effect of imperfections should be a major concern in the design. However, the study of imperfection is complicated for even the simplest of systems. Thus, for this project only imperfections in the initial geometry have been analyzed. The initial imperfections of the system are represented by θ_{01}, θ_{02}. The equations of Equilibrium have to be modified as shown:

$$3(Sin\theta_1 - Sin\theta_{01}) + (Sin\theta_2 - Sin\theta_{02}) - 3pTan\theta_1 = 0 \rightarrow (7)$$
$$(Sin\theta_1 - Sin\theta_{01}) + (Sin\theta_2 - Sin\theta_{02}) - pTan\theta_2 = 0 \quad \rightarrow (8)$$
$$\text{where}: p = P/(KL)$$

The Hessian matrix used here is the same as that used in the case having no initial imperfections. The program algorithm used in this case is also the same. However, here the computations have to be started from p=0, initial $\theta_1 = \theta_{01}$ and initial $\theta_2 = \theta_{02}$. The following cases of initial imperfection have been considered for the given system.

1. $(\theta_{01}, \theta_{02})$ =(0.005, -0.005)
2. $(\theta_{01}, \theta_{02})$ =(0.05, -0.05)
3. $(\theta_{01}, \theta_{02})$ =(0.01, 0.1)
4. $(\theta_{01}, \theta_{02})$ =(0.1, 0.01)
5. $(\theta_{01}, \theta_{02})$ =(0.05, 0.05)

The computations for these have been presented in Tables 3 to 7. The Bifurcation Diagrams for imperfections 1 and 2 have been plotted in figure 6 and for imperfections 3, 4 and 5 have been plotted in figures 7 and 8. All equilibrium paths have been plotted along side Branch 1 (from the case with no initial imperfections).

Imperfection 1:

Arclength	0.05	Initial p	0
Initial θ_1	0.005	Initial θ_2	-0.005

N	θ_1	θ_2	*p*	λ_2	λ_1
1	0.005	-0.005	0	0	0
2	0.0056	-0.0059	0.05	3.2793	0.5207
3	0.0063	-0.007	0.1	3.1454	0.4547
4	0.0073	-0.0086	0.1499	3.0125	0.3876
5	0.0087	-0.0109	0.1999	2.8808	0.3195
6	0.0109	-0.0145	0.2497	2.7505	0.2503
7	0.0148	-0.0211	0.2991	2.6224	0.1804
8	0.0232	-0.0355	0.3462	2.5006	0.112
9	0.0415	-0.0671	0.3805	2.4097	0.0599
10	0.0653	-0.1085	0.395	2.3641	0.0339
11	0.09	-0.1517	0.4007	2.3361	0.0183
12	0.1146	-0.1952	0.4027	2.313	0.0058
13	0.1389	-0.2388	0.4027	2.2906	-0.0062
14	0.163	-0.2826	0.4014	2.2674	-0.0188
15	0.1867	-0.3266	0.399	2.2428	-0.0324
16	0.21	-0.3707	0.3958	2.2167	-0.0474
17	0.2327	-0.4151	0.3918	2.189	-0.064
18	0.2548	-0.4597	0.3871	2.1599	-0.0826
19	0.2761	-0.5046	0.3817	2.1299	-0.1033
20	0.2966	-0.5498	0.3756	2.0992	-0.1265
21	0.3162	-0.5953	0.3689	2.0686	-0.1525

Table 3: Results of computation for imperfection 1

Imperfection 2:

ArcLength	0.05	Initial *p*	0
Initial θ_1	0.05	Initial θ_2	-0.05

N	θ_1	θ_2	*p*	λ_2	λ_1
1	0.05	-0.05	0	0	0
2	0.0555	-0.0584	0.049	3.2763	0.5208
3	0.0625	-0.0693	0.0973	3.1447	0.4563
4	0.0716	-0.0838	0.1443	3.0164	0.3922
5	0.0836	-0.1032	0.1888	2.8936	0.3296
6	0.0991	-0.1289	0.2287	2.7805	0.2709
7	0.1182	-0.1612	0.2618	2.6817	0.2191
8	0.1399	-0.1985	0.287	2.599	0.1754
9	0.1631	-0.239	0.3049	2.5301	0.139
10	0.1869	-0.2812	0.3173	2.4709	0.1077
11	0.2108	-0.3244	0.3256	2.4179	0.0796
12	0.2344	-0.3681	0.3308	2.3687	0.0532
13	0.2576	-0.4123	0.3336	2.322	0.0274
14	0.2803	-0.4568	0.3345	2.2766	0.0015
15	0.3024	-0.5017	0.3339	2.2324	-0.0252
16	0.3236	-0.5469	0.3319	2.1891	-0.0532

17	0.3439	-0.5925	0.3287	2.1469	-0.0832
18	0.3632	-0.6385	0.3244	2.1063	-0.1156
19	0.3812	-0.6848	0.319	2.0679	-0.1511
20	0.3978	-0.7315	0.3127	2.0325	-0.1907
21	0.4127	-0.7787	0.3053	2.0012	-0.2353

Table 4: Results of computation for imperfection 2

Imperfection 3:

ArcLength	0.05	Initial p	0
Initial θ_1	0.01	Initial θ_2	0.1

N	θ_1	θ_2	p	λ_2	λ_1
1	0.01	0.1	0	0	0
2	0.0079	0.1074	0.0494	3.2778	0.5182
3	0.005	0.1167	0.0985	3.1456	0.4524
4	0.0007	0.1285	0.1468	3.0158	0.3861
5	-0.0058	0.1442	0.1939	2.89	0.32
6	-0.0154	0.1658	0.2379	2.7715	0.2559
7	-0.0295	0.1951	0.276	2.6671	0.1972
8	-0.0478	0.2316	0.3048	2.5834	0.1484
9	-0.0689	0.2726	0.324	2.5201	0.1097
10	-0.0911	0.3158	0.3361	2.4711	0.0784
11	-0.1135	0.3599	0.3432	2.4307	0.0513
12	-0.1357	0.4046	0.3468	2.3954	0.0261
13	-0.1575	0.4496	0.348	2.363	0.0013
14	-0.1787	0.4948	0.3472	2.3324	-0.0239
15	-0.1991	0.5404	0.3448	2.3033	-0.0504
16	-0.2187	0.5863	0.341	2.2754	-0.0789
17	-0.2372	0.6324	0.336	2.2491	-0.1101
18	-0.2547	0.6789	0.3299	2.2247	-0.1447
19	-0.2708	0.7257	0.3227	2.2028	-0.1834
20	-0.2856	0.7727	0.3144	2.1841	-0.2273
21	-0.2988	0.82	0.305	2.1694	-0.2775

Table 5: Results of computation for imperfection 3

Imperfection 4:

ArcLength	0.05	Initial p	0
Initial θ_1	0.1	Initial θ_2	0.01

N	θ_1	θ_2	p	λ_2	λ_1
1	0.1	0.01	0	0	0

2	0.1079	0.0022	0.0488	3.2644	0.5214
3	0.1176	-0.0083	0.0966	3.131	0.4575
4	0.1298	-0.0229	0.1429	3.001	0.3944
5	0.1451	-0.0428	0.1862	2.8769	0.3337
6	0.164	-0.069	0.2243	2.7628	0.2778
7	0.186	-0.1013	0.2555	2.6622	0.2289
8	0.2102	-0.138	0.2793	2.5758	0.1878
9	0.2354	-0.1775	0.2967	2.5009	0.1529
10	0.261	-0.2186	0.3092	2.434	0.1226
11	0.2867	-0.2606	0.3178	2.3719	0.095
12	0.3122	-0.3032	0.3237	2.3128	0.0691
13	0.3375	-0.3462	0.3273	2.2551	0.0438
14	0.3624	-0.3895	0.3291	2.198	0.0187
15	0.3868	-0.4332	0.3294	2.1409	-0.0069
16	0.4107	-0.4771	0.3284	2.0837	-0.0332
17	0.4339	-0.5213	0.3264	2.0264	-0.0607
18	0.4563	-0.5659	0.3234	1.9692	-0.0897
19	0.4777	-0.6109	0.3194	1.9124	-0.1205
20	0.498	-0.6564	0.3147	1.8569	-0.1536
21	0.517	-0.7023	0.3091	1.8034	-0.1897

Table 6: Results of computation for imperfection 4

Imperfection 5:

ArcLength	0.05	Initial *p*	0
Initial θ_1	0.05	Initial θ_2	0.05

N	θ_1	θ_2	*P*	λ_2	λ_1
1	0.05	0.05	0	0	0
2	0.0631	0.0598	0.0473	3.2795	0.523
3	0.0669	0.0588	0.0971	3.1446	0.4569
4	0.0717	0.0567	0.1468	3.0107	0.39
5	0.0779	0.0525	0.1963	2.878	0.3223
6	0.0865	0.0445	0.2449	2.7478	0.2545
7	0.0993	0.0293	0.2907	2.6237	0.1892
8	0.1184	0.0026	0.3285	2.5175	0.1336
9	0.1423	-0.0338	0.3531	2.4402	0.0946
10	0.1677	-0.0745	0.3672	2.3844	0.0682
11	0.1935	-0.1165	0.3754	2.3392	0.0481
12	0.2192	-0.1592	0.38	2.2984	0.0309
13	0.2448	-0.2021	0.3822	2.2589	0.0148
14	0.2701	-0.2452	0.3828	2.2193	-0.0013
15	0.2952	-0.2884	0.3821	2.1786	-0.0178
16	0.32	-0.3318	0.3804	2.1363	-0.0353
17	0.3444	-0.3753	0.3778	2.0925	-0.0539

18	0.3684	-0.4191	0.3744	2.047	-0.0738
19	0.3917	-0.4631	0.3702	2	-0.0953
20	0.4144	-0.5074	0.3654	1.9517	-0.1185
21	0.4363	-0.552	0.36	1.9027	-0.1437

Table 7: Results of computation for imperfection 5

DISCUSSION ON THE RESULTS OF IMPERFECTIONS

1. All the imperfections considered here seem to take up equilibrium paths resembling the path of the first buckling mode (branch 1).
2. The first two imperfections have been considered to observe the effect of imperfections in the initial geometry on the load capacity of the structure. The maximum capacity reduces from 0.423KL in the perfect case to 0.4027KL in case of imperfection 1 (5% reduction) and to 0.3345KL in case of imperfection 2 (20% reduction).
3. The imperfections 3, 4 and 5 have been chosen to observe how the direction of imperfection affects the path and load capacity of the system. The interesting feature about these imperfections is that though they initially resemble the second buckling mode shape, they end up tracing a path similar to that of the first buckling mode. Since the bifurcation points are so far apart, it can be speculated that the chances of the imperfections tracing a path similar to that of the second buckling mode are remote.
4. When the maximum loads of imperfections 2 (0.3345KL) and 5 (0.3822KL) are compared, it can be seen that for the same values of imperfections, the load capacity of the structure is higher if the initial geometry resembles the second buckling mode shape. Thus, imperfections resembling the first buckling mode shape are more critical.

5. When the maximum loads of imperfections 3 (0.348KL) and 4 (0.3291KL) – both resembling second buckling mode shape – are compared, it can be seen that the load capacity is greater if $\theta_{01} < \theta_{02}$.

CONCLUSION

Static stability analysis of the chosen two degree of freedom system has been carried out and the results presented in the form of Bifurcation Diagrams and tables of eigen values of the stability matrix. The maximum load for which the system is stable in the straight configuration has been calculated to be 0.423KL. The effect of imperfections on the stability and on the load capacity of the structure has also been analyzed. It has been found that for some cases of imperfection, the behavior of the system is completely different from that suggested by intuition, thus emphasizing the importance of computation in the stability analysis of structures.

REFERENCES

Keith D. Hjelmstad, *Fundamentals of structural mechanics*

APPENDIX

Matlab figures

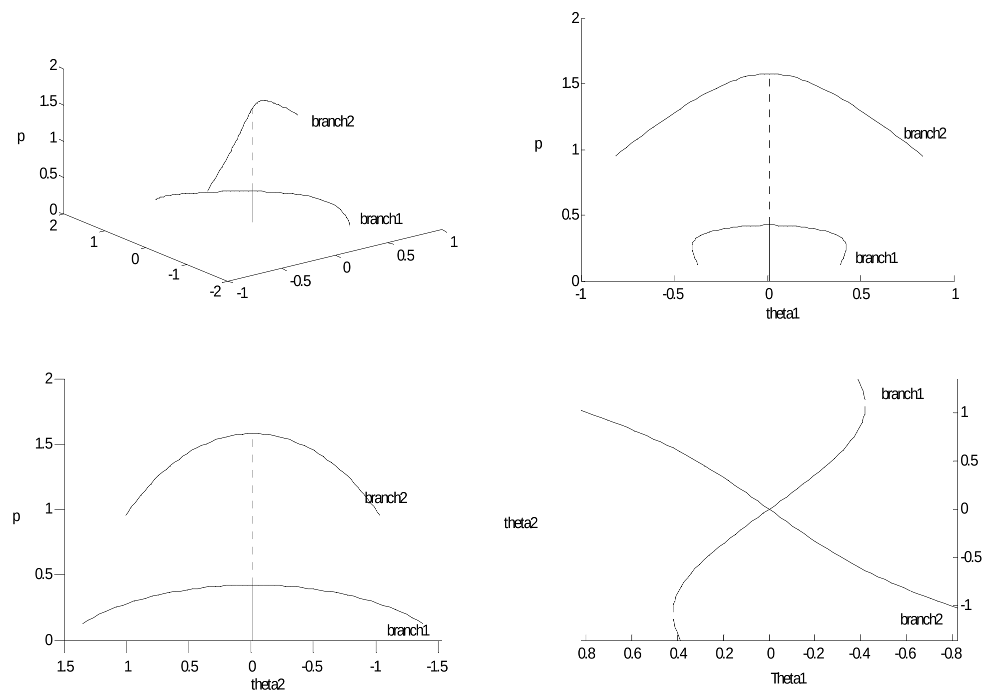

Fig 5: Bifurcation Diagram for no Imperfections in the Initial Geometry

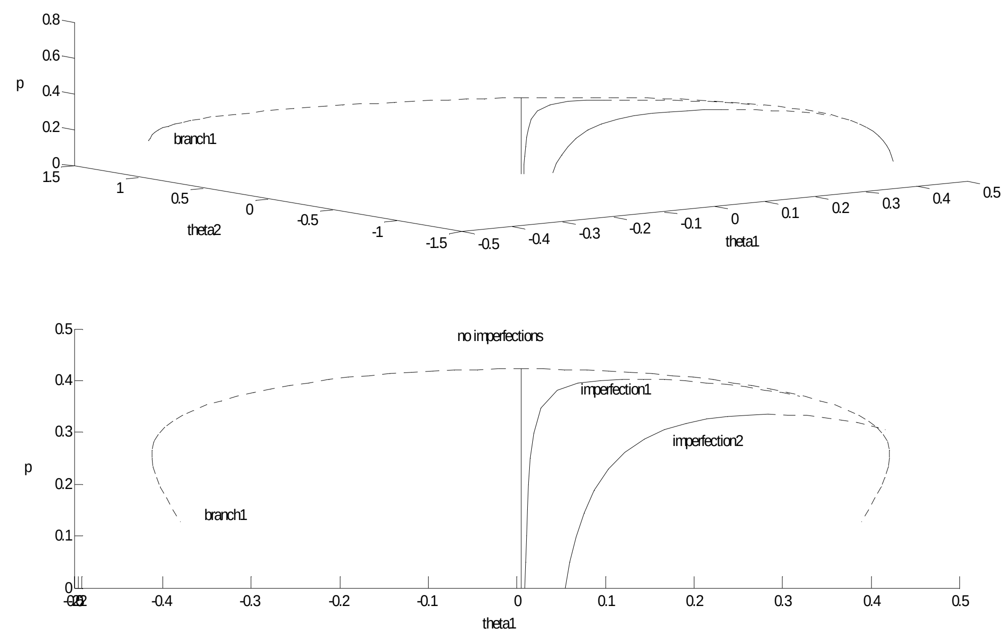

Fig 6: Bifrucation Diagram for structure having initial geometric imperfections.

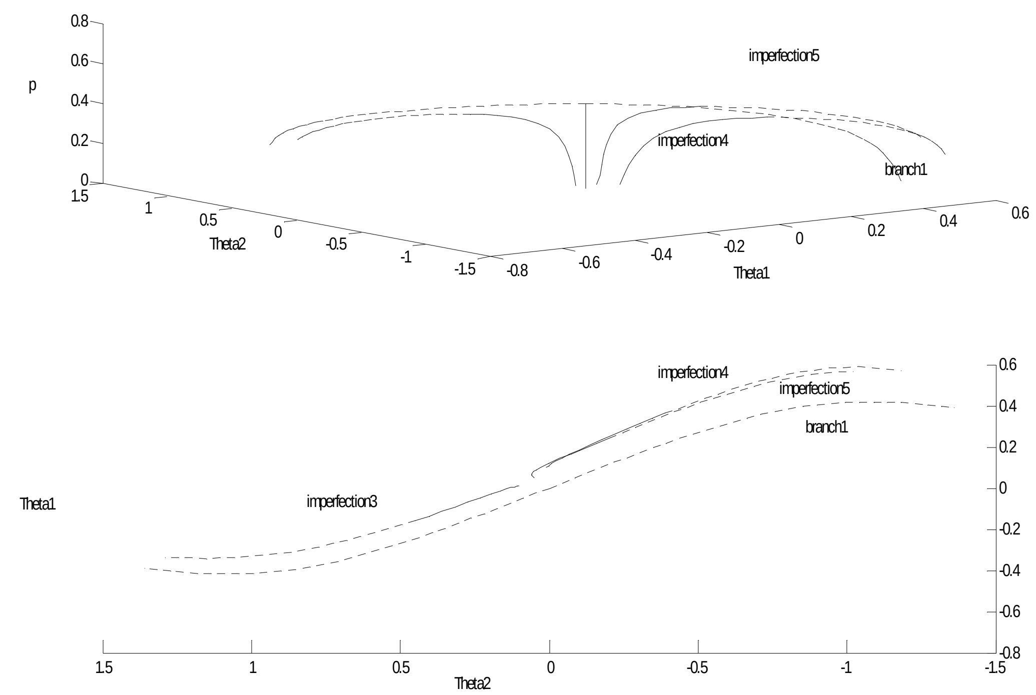

Fig 7: Bifurcation Diagram for structure having initial geometric imperfections

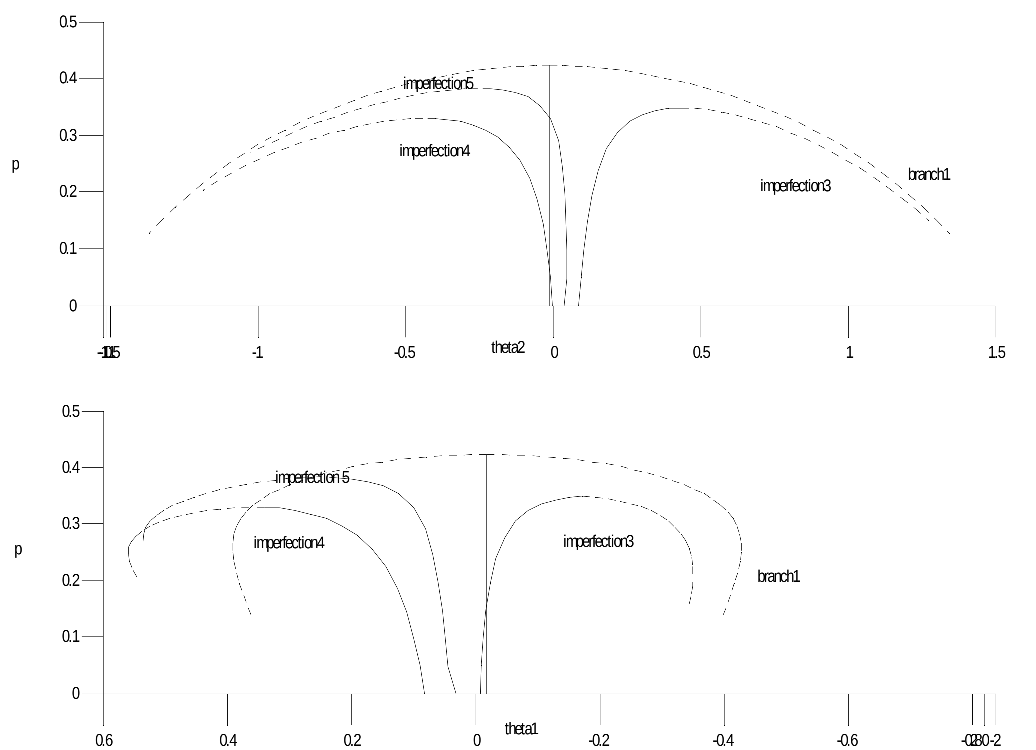

Fig 8: Side views of Bifurcation Diagram in figure 7.